

# Anomalous SZ Contribution to 3 Year WMAP Data

R.M. Bielby\* and T. Shanks

*Department of Physics, Durham University, South Road, Durham, DH1 3LE, UK*

Draft document: 17th March 2007

## ABSTRACT

We first show that the new WMAP 3 year data confirm the detection by Myers et al. (2004) of an extended SZ signal centred on 606 Abell clusters with richness class,  $R \geq 2$ . We also detect SZ decrements around APM and 2MASS groups at increased significance than previously. We then follow the approach of Lieu et al. (2006) and compare the stacked WMAP results for the decrement in 31 clusters with ROSAT X-ray profiles where Lieu et al found on average less SZ decrement in the WMAP 1 year data than predicted. We confirm that in the 3 year data these same clusters also show less SZ decrement than the X-ray data predicts. We then analysed the WMAP results for the 38 X-ray clusters with OVRO/BIMA measured SZ decrements as presented by Bonamente et al. (2006). We again find that the average decrement is measured to be significantly less ( $5.5\sigma$ ) than predicted by the Chandra X-ray data. These X-ray data cause us to re-interpret our previous result; rather than seeing too much SZ at large scales, we may actually be seeing too little SZ decrement near the cluster centre. One possible explanation is that there is contamination of the WMAP SZ signal by radio sources in the clusters but we argue that this appears implausible. We then consider the possibility that the SZ decrement has been lensed away by foreground galaxy groups. Such a model predicts that the SZ decrement should depend on cluster redshift. This effect is clearly detected in the ACO cluster sample and also by comparing the samples of Lieu et al. (2006) and Bonamente et al. (2006). But the mass power-spectrum would require a far higher amplitude than currently expected if lensing was to explain the SZ deficit in high redshift clusters.

**Key words:** cosmology: cosmic microwave background – galaxies: clusters.

## 1 INTRODUCTION

Myers et al. (2004) made a cross-correlation analysis between galaxy cluster catalogues and the WMAP first year data (Hinshaw et al. 2003). They saw a statistical decrement near groups and clusters as detected by APM and also in more nearby groups and clusters as detected by 2MASS but the strongest signal was seen in the ACO rich cluster catalogue. There the decrement was approximately what was expected from predictions based on X-ray observations of the Coma cluster which is itself a richness class 2 cluster. However, the profile appeared to be more extended than expected from simple fits to these typical cluster X-ray data. The extent of the SZ effect, possibly to  $\theta \approx 1$  degree, led Myers et al. (2004) to speculate whether the SZ effect could contaminate the measurement of the acoustic peaks, although the difference between the SZ and primordial CMB spectral indices may constrain such a possibility at least for the first peak (Huffenberger et al. 2004). We now return to

this topic with the first aim to see if the extended SZ effect reproduces in the 3-year WMAP data.

Meanwhile, Lieu et al. (2006) analysed the WMAP first year data now focussing only on 31 clusters with ROSAT X-ray data. They made basic predictions for the SZ decrement in each cluster and found that they overpredicted the SZ decrement. One possibility was that discrete radio sources in the clusters were diluting the decrements but this was argued against by Lieu et al. (2006). However, Lieu & Quenby (2006) also suggested another mechanism which was that synchrotron radiation for CR electrons moving in the cluster magnetic field may form a diffuse cluster radio source which again may dilute the SZ effect. This model was also aimed at explaining the soft X-ray excesses detected in some clusters via inverse Compton scattering of the CMB by the same CR electrons in the cluster (e.g. Nevalainen et al. 2003 and references therein).

Here we shall check the result of Lieu et al. (2006) using our cross-correlation methodology and the full WMAP 3-year data. In the first instance, we shall take the X-ray models of Lieu et al. (2006) which follow the simple  $\beta$  model

\* E-mail:r.m.bielby@durham.ac.uk

**Table 1.** Properties of the WMAP frequency bands.

Band	Frequency	FWHM
W	94GHz	12. <sup>6</sup>
V	61GHz	19. <sup>8</sup>
Q	41GHz	29. <sup>4</sup>
Ka	33GHz	37. <sup>2</sup>
K	23GHz	49. <sup>2</sup>

prescription described in Section 3 below. We shall also look at a new sample of clusters with excellent Chandra X-ray data (Bonamente et al. 2006). Again we shall simply take their models convolved for the WMAP PSF in the appropriate band and compare to the averaged SZ decrement seen in the WMAP3 data.

## 2 DATA

### 2.1 WMAP Third Year Data

For the purpose of the cross-correlations performed here, we use the WMAP 3-year data release (Hinshaw et al. 2006). The WMAP team provide maps in 5 frequency bands (Table 1) plus an internal linear combination (ILC) map from a combination of all five bands. Various masks are also made available by the WMAP team and here we use the Kp mask, which masks much of the galactic contamination from the maps. The cosmological dipole has already been removed from all of the maps. We use the data as provided in the HEALPix format of equal area data elements. Thus, the WMAP data used here is handled in the high resolution HEALPix array characterised by  $N_{side}=512$ , giving a full sky pixel count of 3,145,728 pixels and an element width of  $\sim 7'$ .

### 2.2 Cluster Data

#### 2.2.1 ACO

The ACO catalogue (Abell, Corwin & Olowin 1989) lists clusters with 30 or more members, given the requirements that all members are within 2 magnitudes of the third brightest cluster member, whilst also lying within a  $1.5 h^{-1}$  Mpc radius. A richness class,  $R$ , is applied to the individual clusters based on a scale of  $0 \leq R \leq 5$ . The catalogue covers both hemispheres and here we trim these samples such that we take clusters of only  $R \geq 2$  and galactic latitudes of  $|b| \geq 40^\circ$ .

#### 2.2.2 APM

We shall also use galaxy group and cluster catalogues derived from the APM Galaxy Survey of Maddox et al. (1990) which covers the whole area with  $\delta < -2.5$  deg and  $b < -40$  deg. These were identified using the same ‘friends-of-friends’ algorithm as Myers et al. (2003) and references therein. Circles around each APM galaxy with  $B < 20.5$  are ‘grown’ until the overdensity,  $\sigma$ , falls to  $\sigma = 8$  and those galaxies whose circles overlap are called groups. The APM galaxy surface density is  $N \approx 750 \text{ deg}^{-2}$  at  $B < 20.5$ . Minimum memberships,  $m$ , of  $m \geq 7$  and  $m \geq 15$  were used.

The sky density of groups and clusters is  $3.5 \text{ deg}^{-2}$  at  $m \geq 7$  and  $0.35 \text{ deg}^{-2}$  at  $m \geq 15$ . We assume an average redshift of  $z = 0.1$  for both APM samples.

#### 2.2.3 2MASS

The third cluster catalogue is derived from the final data release of the 2MASS Extended Source Catalogue (XSC) (Jarrett et al. 2000) to a limit of  $K_s \leq 13.7$ .  $K$ -selected galaxy samples are dominated by early-type galaxies which are the most common galaxy-type found in rich galaxy clusters. Therefore the 2MASS survey provides an excellent tracer of the high density parts of the Universe out to  $z < 0.15$  and so provides a further test for the existence of the SZ effect. Using the above 2-D friends-of-friends algorithm, Myers et al. (2004) detected 500 groups and clusters with  $m \geq 35$  members at the density contrast  $\sigma = 8$  in the  $|b| \geq 10$  deg area. The 2MASS groups have average redshift,  $z \approx 0.06$ .

#### 2.2.4 ROSAT X-ray cluster sample

We also analyse the 31 clusters published by Bonamente et al. (2002). This cluster sample was originally selected as a sample of X-ray bright clusters suitable for observation of the X-ray surface brightness profiles. X-ray profiles were obtained with the ROSAT PSPC instrument and estimates of the gas temperature, density and distribution were made fitting a  $\beta$  profile model to the data. The X-ray data for these 31 clusters were previously used by Lieu et al. (2006) to construct predictive models of the SZ profile of each cluster. Redshifts for these clusters range from  $z \sim 0.02$  (Coma) up to  $z \sim 0.3$  (Abell 2744), whilst the sample lies in the galactic latitude range of  $|b| \geq 25^\circ$ .

#### 2.2.5 Chandra X-ray cluster sample

We further analyse the 38 clusters discussed by Bonamente et al. (2006). These clusters have been observed at 30GHz by OVRO and BIMA (see Bonamente et al. (2006) and references therein) to detect the SZ decrements and have also been observed by Chandra to provide the X-ray data needed to estimate the value of  $H_0$ . The interferometric radio observations have a resolution of  $\approx 1'$  and the X-ray observations from the Chandra ACIS-I camera have a resolution of  $\approx 1''$ . Redshifts for these clusters are in the range  $0.18 < z < 0.8$ , a higher range than for the ROSAT sample. Bonamente et al. (2006) fitted  $\beta$  models to the X-ray data and made predictions for the SZ decrements.

## 3 SZ X-RAY MODELLING

The SZ effect is generally modelled using X-ray gas profiles, densities and temperatures. The X-ray data is most simply modelled by fitting a  $\beta$  model to the X-ray intensity profile:

$$S_X = S_{X0} \left(1 + \frac{r^2}{r_c^2}\right)^{(1-6\beta)/2} \quad (1)$$

where  $S_{X0}$  is the central X-ray surface brightness and  $r_c$  is the core radius. The temperature decrement,  $\Delta T_{SZ}$ , as a

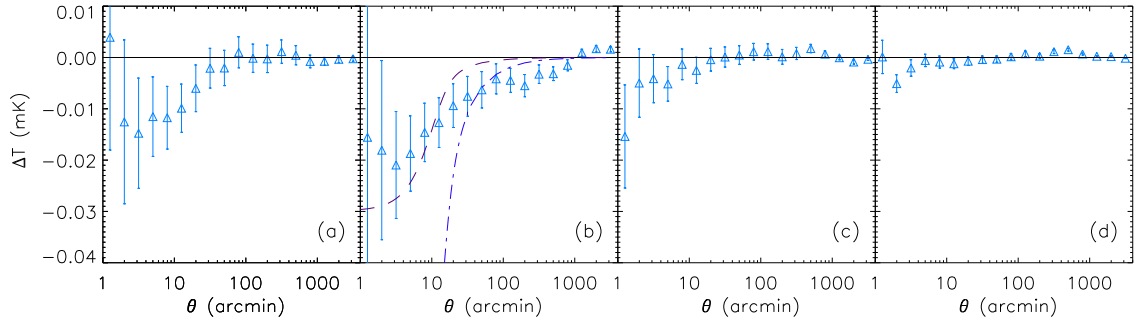


**Figure 1.** Cross-correlation results between the WMAP 3-year W-band temperature data and the four cluster datasets: (a) 2MASS, (b) ACO, (c) APM  $m \geq 15$ , and (d) APM  $m \geq 7$ . The dashed and dot-dashed lines in (b) show SZ models with  $\Delta T = 0.083K$  and  $\Delta T = 0.49K$  respectively, both with  $\theta_c = 1.5$  and  $\beta = 0.75$  and convolved with the WMAP beam-width. The latter model is intended to be representative of the Coma cluster, scaled to redshift  $z = 0.15$ . The former is the ACO model fitted by Myers et al. (2004) in their analysis of the WMAP 1st year results.

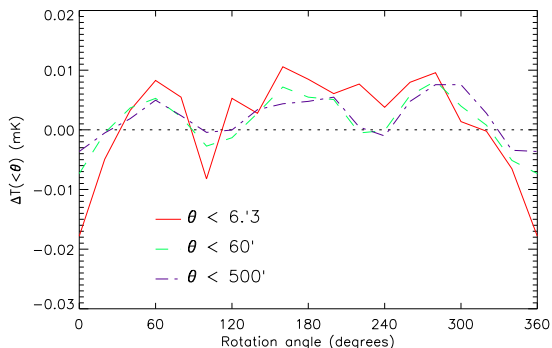


**Figure 2.** The cross-correlation of the ACO catalogue is shown after increments in galactic longitude of 20deg in the Abell cluster positions. The mean  $\Delta T$  is shown for WMAP pixels within 6.3', 60' and 500' of cluster centres, where the significance at each angular limit is  $3.15\sigma$ ,  $2.00\sigma$  and  $1.16\sigma$  respectively.

function of the angular distance from the cluster-centre,  $\theta$ , is given by equation 2.

$$\Delta T_{SZ}(\theta) = \Delta T_{SZ}(0) \left[ 1 + \left( \frac{\theta}{\theta_c} \right)^2 \right]^{-\frac{3\beta}{2} + \frac{1}{2}} \quad (2)$$

where  $\theta_c = r_c/D_A$  and  $D_A$  is the angular diameter distance of the cluster. The magnitude of the central temperature shift,  $\Delta T_{SZ}(0)$ , is given by equation 3.

$$\frac{\Delta T_{SZ}(0)}{T_{CMB}} = \frac{kT_e}{m_e c^2} \sigma_{Th} n_o \left[ \frac{x(e^x + 1)}{e^x - 1} - 4 \right] \quad (3)$$

where  $x = h\nu/kT_e$ ,  $\sigma_{Th}$  is the Thomson cross-section and  $n_o$ ,  $T_e$  are the central gas density and the temperature derived from the X-ray data. Lieu et al. (2006) use the cluster sample of Bonamente et al. (2002) and fit ROSAT PSPC cluster X-ray profiles. They assume isothermal gas distributions with  $T_e$  taken from Bonamente et al. (2002). Bonamente et al. (2006) use hydrostatic equilibrium models allowing a double power-law for the number density run with radius to make the SZ predictions. They allow the gas temperature to vary with radius and a CDM component as well as gas to contribute to the cluster potential. We shall simply assume the models of Lieu et al. (2006) and

Bonamente et al. (2006) and convolve the predicted SZ profile with the appropriate WMAP beam profile, modelled as a Gaussian with the FWHM beamwidth shown in Table 1.

#### 4 CROSS-CORRELATION ANALYSIS

We focus our analysis on the 94GHz W band from WMAP, looking for correlations characteristic of the SZ effect in this, the highest resolution band. We perform a cross-correlation analysis as described in Myers et al. (2004), calculating the mean temperature decrement/increment as a function of angular separation from galaxy clusters in the above datasets.

$$\delta T_c(\theta) = \sum_i \frac{\delta T_i(\theta)}{n_i} \quad (4)$$

We estimate the errors on our results using repeated Monte Carlo realisations of the cluster data. For each cluster dataset, we create 100 mock catalogues containing the number of clusters of the parent catalogue. We also incorporate the clustering of the parent catalogue in each case. For each realisation we create  $5 \times$  the number of clusters required. We then calculate a clustering amplitude for each individual cluster and attribute a weighting based on the assigned clustering amplitude. Clusters are then selected or discarded based on their weighting, until the realisation has the required number of clusters (i.e. that of the parent catalogue). As a final check, the auto-correlation of the realisation is measured. This is then compared to the auto-correlation of the original catalogue. If the autocorrelation amplitude is not within required limits, the realisation is discarded and the process is begun anew.

Once a hundred realisations have been acquired, the cross-correlation is calculated between the WMAP data and each realisation. The  $1\sigma$  error is then estimated as the standard deviation calculated from the 100 realisation cross-correlations.

## 5 RESULTS

### 5.1 Optical/IR Cluster Samples

The results for the cross-correlation between the four large cluster datasets (APM  $m \geq 7$ , APM  $m \geq 15$ , ACO  $R \geq 2$  and

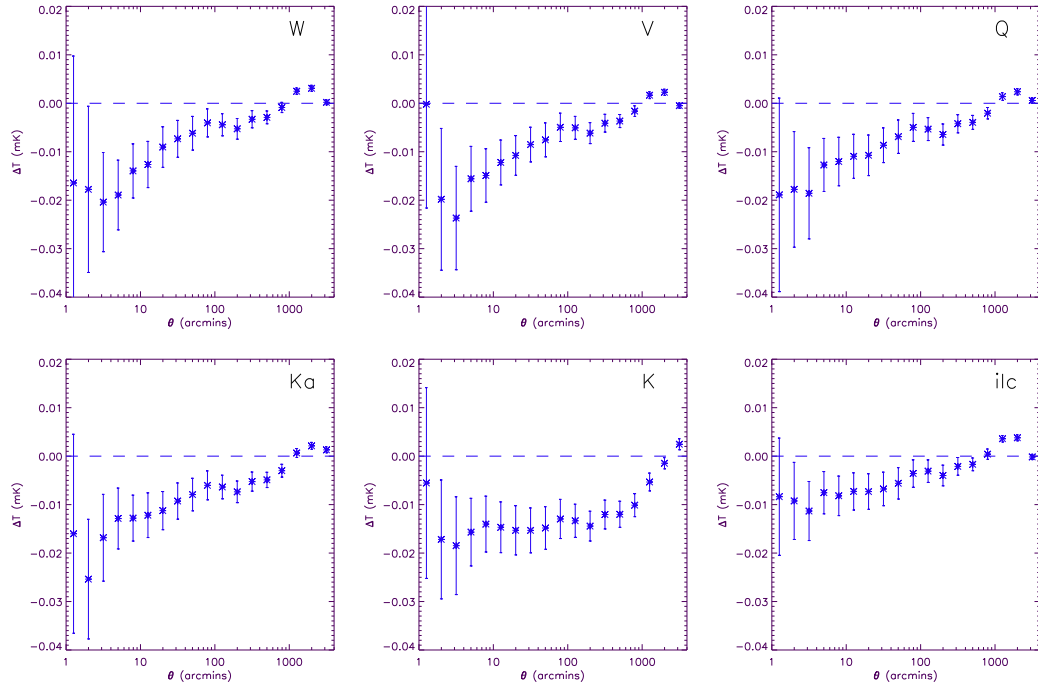


**Figure 3.** Cross-correlation results between 606 ACO rich galaxy clusters ( $R \geq 2$ ,  $|b| > 40\text{deg}$ ) and the WMAP 3-year maps in 5 bandpasses (+ILC) as indicated.

2MASS clusters) and the WMAP W-band data are shown in Fig. 1. A decrement is immediately evident on small scales within  $\theta < 30'$  of cluster centres in all four data sets. Looking in detail first at the ACO results, the WMAP3 cross-correlation strongly confirms the results of Myers et al. (2004) from WMAP 1st year data. Here, we find a decrement of  $-0.021 \pm 0.007mK$  at  $\theta < 6'.3$  and  $-0.010 \pm 0.004mK$  at  $\theta < 60'$  for the W-band data (quoted accuracies are from the Monte-Carlo analysis). Basically, the ACO decrement has remained the same and the improved statistics at small angles has increased the S/N. In addition to the Monte-Carlo analysis, we also checked our ACO results using the rotational analysis described by Myers et al. (2004) and find the significance of the decrement at  $6'.3$ ,  $60'$  and  $500'$  to be  $3.15\sigma$ ,  $2.00\sigma$  and  $1.16\sigma$  (see Fig. 2). As before, there appears to be some form of extended signal out to angles of  $\sim 100'$ . Following Myers et al. (2004), we also produce the correlations with the four other WMAP bands, plus the ILC map. The results of this are shown in Fig. 3. Again, good agreement is seen between these updated results and the original 1st year data results. Despite the increasingly poorer resolution of the bands, the decrement is observed in the V, Q and Ka bands, whilst even the ILC map and the Ka band map show a decrement.

Improvements in the small scale statistics are also observed in the 2MASS and APM results while the magnitudes of the decrements remain unchanged. However, the APM group ( $m \geq 7$ ) SZ detections remain marginal even at small scales.

## 5.2 ROSAT X-ray bright cluster sample

We next consider the X-ray bright clusters of Bonamente et al. (2002). Analysis of this dataset with respect to the first year WMAP results has already been performed by Lieu et al. (2006). Their main conclusion was that the SZ decrement in the WMAP1 data around the locations of these clusters has a lower magnitude than they would expect from their predictions based on the original X-ray observations of Bonamente et al. (2002). In Fig. 4 (left panel) we show our cross-correlation between the 31 clusters used by Lieu et al. (2006) and the WMAP year 3 data in the W-band. We also present the average model prediction based on the Bonamente et al. (2002) data. This has been convolved with a Gaussian beam profile of  $\sigma = 6'.3$ . We see the same general effect as seen by Lieu et al. (2006), that the SZ effect is somewhat smaller than predicted by the data. However, the significance of rejection is only  $\approx 2\sigma$ . Similar results are seen in the other WMAP bands.

We next split the Lieu et al. (2006) clusters by galactic latitude to see if the SZ effect was diluted by foreground contamination at low galactic latitudes. Fig. 5 (upper panels) shows that there is some evidence in the W band at least that the low latitude clusters look to have smaller decrements than the higher latitude clusters. The significance of rejection of the model value for a bin at  $\theta < 6'.3$  are  $2.3\sigma$  for  $|b| \geq 40\text{deg}$  and  $4.1\sigma$  for  $20\text{deg} \leq |b| \leq 40\text{deg}$ . We also divided the ROSAT data by redshift, splitting the data at  $z = 0.1$  (Fig. 5 lower panels). The higher redshift clusters here give somewhat better model fits.

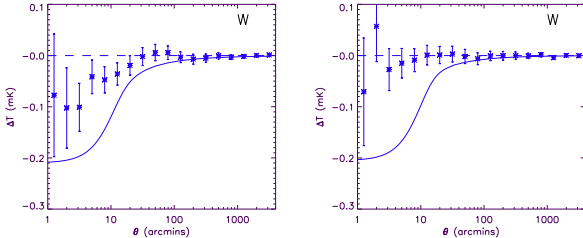


**Figure 4.** Average  $\Delta T$  (from WMAP W-band data) plots for 30 clusters from the ROSAT sample (left) and 39 clusters from the Chandra sample (right).

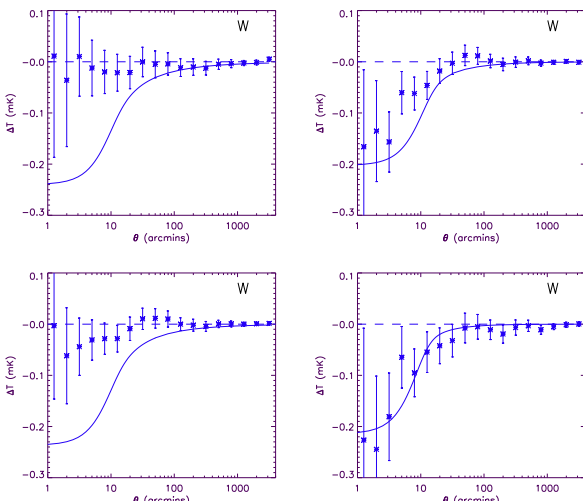


**Figure 5.** Average  $\Delta T$  (from WMAP W-band data) plots for the ROSAT X-ray clusters. Plotted at top are the correlation with 11 clusters at  $b < 40^\circ$  (left) and 19 at  $b > 40^\circ$  (right). Plotted at bottom are the correlation with 21 clusters at  $z < 0.1$  (left) and 9 at  $z > 0.1$  (right).

### 5.3 Chandra X-ray bright cluster sample

We next analysed the SZ decrements for the 38 clusters of Bonamente et al. (2006), using the WMAP3 W band results. In Fig. 4 (right panel) we compare the cross-correlation results with the hydrostatic equilibrium models of Bonamente et al. (2006) and again find that the the SZ effect is now quite severely over-predicted by the models, with a rejection significance of  $5.5\sigma$ . We again looked for a dependence on galactic latitude and failed to find any (Fig. 6). We also looked for a dependence on redshift, splitting the clusters at  $z = 0.3$ . The lower redshift clusters gave a slightly better fit than the higher redshift clusters but again only marginally.

Although within either the Chandra or ROSAT samples there is little evidence of redshift dependence, the fits of SZ models to the WMAP data do appear to deteriorate as we move from the average redshift,  $z \approx 0.1$  of the Bonamente et al. (2002) sample to  $z \approx 0.3$  of the Bonamente et al. (2006) sample. We have also noted that at the lowest redshift the WMAP SZ effect is clearly detected at about the predicted amplitude in the Coma cluster (Fig. 7). We therefore returned to the ACO dataset and identified

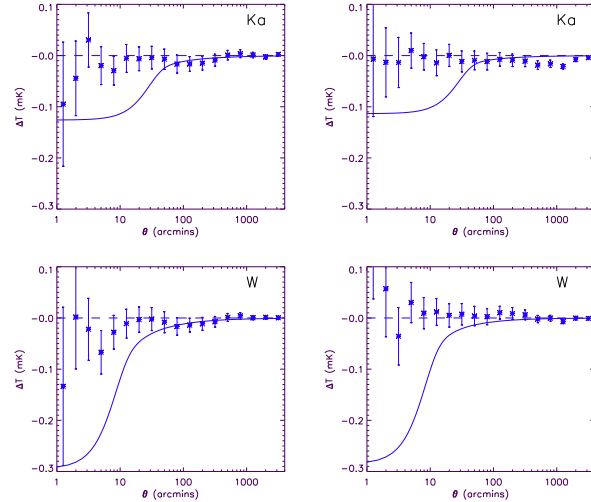


**Figure 6.** Top: Cross-correlations between WMAP Ka-band  $\Delta T$  data with 18 clusters with  $|b| < 40^\circ$  (left) and 21 with  $|b| > 40^\circ$  (right) from the Chandra cluster sample. Bottom: The same for WMAP W-band data.

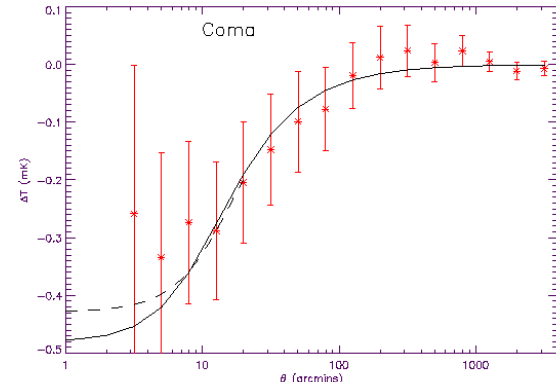


**Figure 7.** Binned  $\Delta T$  data from the WMAP year-3 W-band data around the Coma cluster. The solid line shows the model predicted from X-ray data (taken from Lieu et al. 2006), whilst the dashed line is the model convolved with the W-band beam profile.

407  $R \geq 2$ ,  $|b| > 40$ deg clusters with measured redshifts. Splitting these at  $z=0.15$  (Fig. 8), we see that there is some evidence confirming that clusters at higher redshift have observed SZ decrements that are significantly smaller than at lower redshift. Although the X-ray properties for the majority of these clusters are unknown, we have fitted the same average model, scaling  $\theta_c$  to the appropriate average redshift before convolving with the WMAP beam. The fit appears significantly worse for the higher redshift clusters, with a rejection confidence at  $\theta < 6.3'$  of  $\approx 1\sigma$  for  $z < 0.15$  and  $\approx 4\sigma$  for  $z > 0.15$ . We tentatively conclude that there may be a redshift dependence of the SZ effect in the sense that higher redshift clusters show a smaller than expected effect.

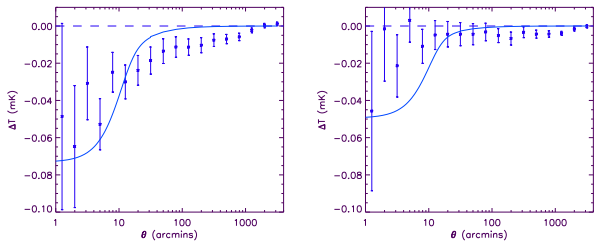


**Figure 8.** Average  $\Delta T$  (from WMAP W-band data) plots for the data from the Abell cluster catalogue with 172 clusters at  $z < 0.15$  (left) and 235 at  $z > 0.15$  (right). Only clusters with  $|b| \geq 40$  deg are included here. Overlaid in both cases is a model with  $\Delta T(0) = -0.16\text{mK}$ ,  $\beta = 0.7$  and  $\theta_c = 9.8'$  scaled to the mean redshift of the samples:  $z = 0.1$  and  $z = 0.2$ . In both cases the model is convolved with the W-band beam profile. This model gives a reasonable fit to the data at  $z < 0.15$ , but significantly overestimates the  $z > 0.15$  data.

## 6 DISCUSSION

The reduced SZ decrements in the WMAP3 data towards the ROSAT cluster sample and the almost lack of detection of the SZ effect in terms of the Bonamente et al. (2006) clusters is paradoxical. The most obvious explanation is that the WMAP data is contaminated by unresolved cluster radio sources within the WMAP beam. However, the arguments against this explanation are that the discrepancy in the WMAP3 data for the Bonamente et al. (2006) cluster sample is as large at Ka (33GHz) as at W (94GHz) (see Fig. 6) and the higher resolution BIMA/OVRO interferometric data at 30GHz did not detect such a population (Coble et al. 2007). Currently we have no explanation for the strong SZ decrements detected by the interferometric experiments as opposed to the lack of detections by WMAP. At higher resolution it may be more possible to detect the SZ against the noise caused by the primordial CMB fluctuations but our error analysis should take care of such statistical effects and the average model is rejected at the  $5.5\sigma$  level by the WMAP data. A high value of  $H_0 \approx 100\text{km}\text{s}^{-1}\text{Mpc}^{-1}$  for the SZ X-ray model might help explain the ROSAT cluster results but an even higher value would be required to explain the Chandra cluster results.

As noted above there may also be evidence that the SZ decrement is too low in the ACO-WMAP1 cross-correlation of Myers et al. (2004), as confirmed by the ACO-WMAP3 cross-correlation in Fig. 1. Myers et al. (2004) noted that the decrement that fitted the ACO  $R \geq 2$  clusters with  $\beta = 0.75$  was only  $\Delta T(0) = 0.083\text{mK}$  compared to the  $0.5\text{mK}$  predicted for the  $R = 2$  Coma cluster. The WMAP3 data confirms that  $\Delta T(0) = 0.5\text{mK}$  is needed to fit the observed Coma SZ decrement (see Fig. 7). In Fig. 1 the SZ models for these two values of the decrement are compared to the WMAP3 W band data for the  $R \geq 2$  cluster sample. Both models assume  $\beta = 0.75$ . We see that while the data is well fitted at  $\theta < 10'$  by the  $\Delta T(0) = 0.083\text{mK}$  model, the  $\Delta T(0) = 0.5\text{mK}$  at least begins to improve the fit at larger scales. One possibility is that instead of (or as well as) detecting an extended SZ component to the ACO data, we are failing to detect the central SZ decrement.

Lieu et al. (2006) discussed other possible explanations for the unexpectedly small SZ decrements detected in the

ROSAT sample. For example, Lieu & Quenby (2006) have discussed whether a diffuse cluster synchrotron source could explain the reduced SZ decrement. The main problem here is that non-thermal electrons would not give a good fit to the X-ray data which are usually well fitted by thermal bremsstrahlung, although Lieu & Quenby (2006) also noted that the soft X-ray excess seen in the central regions of some clusters may be indicative of a significant embedded non-thermal X-ray component there.

Fosalba et al. (2003) have discussed whether ISW effect could mask the SZ effect but the ISW effect is at  $0.5\mu\text{K}$  and seems too small to mask the SZ effect which in the X-ray clusters can be  $10\times$  higher.

There is also the possibility that the SZ decrement has been overestimated by the X-ray modelling. Certainly the Chandra predicted decrements for the 5 clusters in common with the ROSAT sample (A665, A1413, A1689, A1914, A2218) are on average  $\approx 80\%$  larger than the predicted decrements from the ROSAT data. Most of this difference arises from A2218 where the ROSAT data imply  $\Delta T(0) = -0.27\text{mK}$  (corrected to 30GHz) and the Chandra data imply  $\Delta T(0) = -0.87\text{mK}$ , a factor 3.2 different.

While this paper was in preparation, Afshordi et al. (2006) have also used X-ray data of 193 Abell Clusters to search for the SZ decrement from WMAP3 data (see also Afshordi et al. 2005). These authors made a significant detection and also claimed that the WMAP SZ data and also suggested that the size of SZ decrement implied that the cluster hot gas fraction was  $32 \pm 10\%$  lower than the baryon fraction in the standard cosmological model. They also suggested that their WMAP results were consistent with the interferometric SZ results for the sample of 38 Chandra clusters analysed above. Note that the approach of Afshordi et al. (2006) is different from that used here in that the X-ray data is mainly used to define a template to detect SZ decrements and then the SZ data and the X-ray temperature data alone are used to establish the gas densities. This route therefore avoids comparing the SZ results with X-ray gas density models on the grounds that the latter depend on assumptions such as that of hydrostatic equilibrium. These authors also do not consider the possibility that the cluster SZ decrements may evolve with redshift.

Finally, if we assume that the WMAP SZ decrements are reliable, even in the case of the 38 Chandra clusters where the unexplained discrepancy persists with the OVRO/BIMA results of Bonamente et al. (2006), we might speculate whether a lower than expected SZ decrement in the higher redshift clusters could be caused by foreground lensing. The indication from WMAP that the higher redshift clusters may have reduced SZ decrements is consistent with the idea that gravitational lensing is having a significant effect on the detection of the SZ effect. Therefore it may be that the groups and clusters out to redshifts in the range  $0.2 < z < 0.8$  in the foreground of the targeted Chandra clusters are lensing the cluster centres and smoothing the decrement away. Using CMBFAST we have constructed the lensing smoothing function for CMB scattering at  $z = 0.3$  and find that on the size of the  $\approx 10$  arcmin WMAP beam, the smoothing function is reduced by about a factor of  $\approx 10$  compared to the case where the surface of last scattering is at  $z = 1100$ . At  $z = 0.7$ , the factor is  $\approx 5$ . Therefore for the standard model this would make the effect negligi-

ble because at  $z=0.3$ ,  $\epsilon = \sigma/\theta \approx 0.004$  and at  $z = 0.7$ ,  $\epsilon = \sigma/\theta \approx 0.008$ . Only if the mass power spectrum is significantly higher than that for the standard model can this explanation apply. One such case is the high mass power spectrum advocated by Shanks (2006) as a route to modify the first acoustic peak in the CMB. Such a spectrum is motivated by the evidence from QSO lensing that the galaxy distribution is strongly anti-biased ( $b \approx 0.1$ ) at least on  $0.1 - 1 h^{-1} \text{Mpc}$  scales with respect to the mass (Myers et al. 2003, 2005; Mountrichas & Shanks 2007). However, the balance of other evidence may still argue against such a high amplitude for the mass power-spectrum.

Lensing would clearly also affect the X-ray cluster profiles as well as the SZ decrements. Although these are expected to be smoother than the SZ decrements, it might be expected that the profiles of lower redshift clusters are on average steeper than the profiles of higher redshift clusters. It remains to be seen whether this prediction of the lensing hypothesis can be decoupled from evolution of the cluster gas component. In any case, the flatness of the X-ray profiles towards the centres of many clusters may make this prediction more difficult to test.

## 7 CONCLUSIONS

We have confirmed the detection of an extended SZ effect in ACO  $R \geq 2$ , 2MASS and APM clusters. We have also confirmed the result of Lieu et al. (2006) that the SZ decrement is somewhat lower than expected on standard model assumptions and ROSAT X-ray profiles for a sample of 31 clusters from Bonamente et al. (2002). We have further shown that even smaller X-ray decrements are seen in the higher-redshift sample of 38 clusters of Bonamente et al. (2006) that has Chandra X-ray data. The reason for the observational discrepancy between the WMAP data and the BIMA/OVRO data of Bonamente et al. (2006) is not clear. We do not believe that discrete or diffuse cluster radio sources nor the ISW effect is likely to explain the discrepancy. Dividing the ACO clusters into high and low redshift samples also indicates that the deficit in the SZ decrement may increase at higher redshift.

In the light of the above results from our WMAP SZ analysis, we have discussed the possibility that the extended SZ signal detected for ACO and 2MASS clusters is actually indicating a lack of SZ signal in the centres of clusters rather than an excess at the edges.

On the assumption that the WMAP SZ results are correct, one explanation we have considered is that lensing of the cluster centres by foreground groups and clusters could explain the overprediction of the observed decrements by SZ models and in particular the apparent tendency for higher redshift clusters to have smaller SZ decrements.

It will be interesting to see if these results are confirmed in the higher resolution SZ observations made using the Planck satellite. Another prediction is that the X-ray profiles of clusters should get shallower with redshift if the lensing hypothesis is correct.

## ACKNOWLEDGMENTS

We thank R. Lieu and J. Mittaz for useful discussions.

## REFERENCES

Abell G.O., Corwin H. & Olowin R., 1989, ApJS, 70, 1  
 Afshordi N., Loh Y. & Strauss M.A., 2003, AAS 203, 35, 1316  
 Afshordi N., Lin, Y-T & Sanderson, A.J.R. 2005, ApJ, 629, 1  
 Afshordi N., Lin, Y.T., Daisuke, N. & Sanderson, A.J.R. 2006, astro-ph/0612700  
 Bonamente M., Lieu R., Joy M. K. & Nevalainen J.H., 2002, ApJ, 576, 688  
 Bonamente M., Joy M. K., LaRoque S. J., Carlstrom J. E., Reese E. D. & Dawson K. S., 2006, ApJ, 647, 25, 2006, ApJ, 647, 25  
 Coble, K., Carlstrom, J.E., Bonamente, M., Dawson, K., Holzapfel, W., Joy, M., LaRoque, S. & Reese, E.D., astro-ph/0608274  
 Diego J.M., Silk J. & Sliwa W., 2003, MNRAS, 346, 940  
 Fosalba P., Gaztaaga E. & Castander F.J., 2003, ApJ, 597, L89  
 Hinshaw, G. et al., 2003, ApJS, 148, 63  
 Hinshaw G., Nolta M.R., Bennet C.L., Bean R., Dore O., Greason M.R., Halpern M., Hill R.S., Jarosik N., Kogut A., Komatsu E., Limon M., Odegard N., Meyer S.S., Page L., Peiris h.P., Spergel D.N., Tucker G.S., Verde L., Weiland J.L., Wollack E. & Wright E.L., 2006, ApJ in press  
 Huffenberger K.M., Seljak U. & Makarov A., 2004, Phys.Rev.D, 70, 6, 063002  
 Jarrett, T.H., Chester, T., Cutri, R., Schneider, S., Skrutskie, M., Huchra, J.P., 2000, AJ, 119, 2498  
 Lieu R., Mittaz J.P.D. & Zhang S.-N., 2006, ApJ, 648, L176  
 Lieu R. & Quenby J., 2006, ApJ submitted, astro-ph/0607304  
 Maddox, S. J., Efstathiou, G., Sutherland, W. J., Loveday, J. 1990, MNRAS, 243, 692  
 Mountrichas, G. & Shanks, T. 2007, MNRAS, submitted, astro-ph/0701870  
 Myers, A.D., Outram, P.J., Shanks, T., Boyle, B.J., Croom, S.M., Loaring, N.S., Miller, L., Smith, R.J., 2003, MNRAS, 342, 467  
 Myers A.D., Shanks T., Outram P.J., Frith W.J. & Wolfendale A.W., 2004, MNRAS, 347, L67  
 Myers A.D., Outram P.J., Shanks T., Boyle,B.J., Croom,S.M., Loaring,N.S., Miller,L., Smith & R.J., 2005, MNRAS, 359, 741  
 Nevalainen, J., Lieu, R., Bonamente, M., and Lumb, D., 2003, ApJ, 584, 716  
 Refregier A., Spergel D.N. & Herbig T., 2000, ApJ, 531, 31  
 Shanks T., 2006, MNRAS accepted, astro-ph/0609339  
 Sunyaev R.A. & Zel'dovich Y.B., 1980, ARA&A, 18, 537